RSC Advances

PAPER

View Article Online
View Journal | View Issue

Cite this: *RSC Adv.*, 2021, **11**, 20769

A simple and cost-effective paper-based and colorimetric dual-mode detection of arsenic(III) and lead(II) based on glucose-functionalized gold nanoparticles†

Bhuneshwari Sahu, Ramsingh Kurrey, Manas Kanti Deb, * Kamlesh Shrivas, Indrapal Karbhal and Beeta Rani Khalkho

We report a simple and cost-effective paper-based and colorimetric dual-mode detection of As(III) and Pb(II) based on glucose-functionalized gold nanoparticles under optimized conditions. The paper-based detection of As(III) and Pb(II) is based on the change in the signal intensity of AuNPs/Glu fabricated on a paper substrate after the deposition of the analyte using a smartphone, followed by processing with the ImageJ software. The colorimetric method is based on the change in the color and the red shift of the localized surface plasmon resonance (LSPR) absorption band of AuNPs/Glu in the region of 200–800 nm. The red shift ($\Delta\lambda$) of the LSPR band observed was from 525 nm to 660 nm for As(III) and from 525 nm to 670 nm for Pb(II). The mechanism of dual-mode detection is due to the non-covalent interactions of As(III) and Pb(II) ions with glucose molecule present on the surface AuNPs, resulting in the aggregation of novel metal nanoparticles. The calibration curve gave a good linearity range of 20–500 μg L^{-1} and 20–1000 μg L^{-1} for the determination of As(III) and Pb(II) with the limit of detection of 5.6 μg L^{-1} and 7.7 μg L^{-1} for both metal ions, respectively. The possible effects of different metal ions and anions were also investigated but did not cause any significant interference. The employment of AuNPs/Glu is successfully demonstrated for the determination of As(III) and Pb(II) using paper-based and colorimetric sensors in environmental water samples.

Received 15th April 2021
Accepted 27th May 2021

DOI: 10.1039/d1ra02929k

rsc.li/rsc-advances

1. Introduction

Consumption of drinking water contaminated with toxic metals such as arsenic (As) and lead (Pb) has deadly effects on human beings.[1] There are four different types of oxidation states of As (−3, +3, 0, and +5) that are possible to be found in nature, amongst which As(III) is known as the most hazardous one. Exposure to As can cause a variety of diseases, including abdominal pain, vomiting, diarrhea, nausea, depigmentation, hyper pigmentation, keratosis, blackfoot, peripheral vascular disorder, and several types of cancer.[2,3] Pb is another toxic metal found in the crust of earth, water, and soil, and potentially affects almost every system such as reproductive, neurological, hematopoietic, hepatic, and renal in the human body.[4] Pb can even cause cancer owing to its excessive accumulation in the human body.[4] In order to ensure water quality, different regulatory agencies have been set a tolerance limit for these contaminants in water bodies.[5–7] These guidelines define the mandatory quality standards of water intended for human consumption. In India, the ground waters of Chhattisgarh and West Bengal states are exceedingly contaminated with As, which exceed the World Health Organization's (WHO) drinking water guidelines (10 μg L^{-1}).[8] Therefore, the detection of As(III) and Pb(II) in water samples is important to know the mechanism pathway of these pollutants entering into different compartments of the environment.

Several advanced analytical methods exist for the detection of As(III) and Pb(II) in water samples. Among them, UV-Vis spectrophotometry,[5,6] hydride generation-atomic absorption spectrometry,[7,8] graphite furnace-atomic absorption spectrometry,[9,10] inductive coupled plasma hyphenated with atomic emission spectrometry,[11,12] inductively coupled plasma hyphenated with mass spectrometry,[13] atomic fluorescence spectrometry,[14,15] and cyclic voltammetry[16,17] are the most widely used. The advanced instruments are costly, sensitive, have high consumption, require professional operators and other expensive instruments as well as complex sample pretreatment processes. Furthermore, these conventional methods are not economical because heavy metal elements are rarely discovered in the environment during routine inspections.[6–8] Therefore, creating a simple and low-cost approach to meet practically the requirements for the detection of heavy

School of Studies in Chemistry, Pt. Ravishankar Shukla University, Raipur, CG-492010, India. E-mail: debmanas@yahoo.com; Tel: +91 94255 03750

† Electronic supplementary information (ESI) available. See DOI: 10.1039/d1ra02929k

metals in water samples is necessary. A number of colorimetric paper-based analytical devices have been used to detect several chemical substances because these devices provide the characteristics of simplicity, portability, rapidity, disposability, and selectiveness.[18–20] Recently, our research group demonstrated the use of a paper-based and colorimetric sensor for the on-site determination of metal ions using functionalized nanoparticles in environmental and biological samples.[21,22] Apilux *et al.* developed a paper-based sensor for the determination of Hg^{2+} in water samples using silver nanoplates.[23] Ratnarathorn *et al.* developed PADs for the quantitative determination of copper using homocysteine and dithiothreitol-modified AgNPs.[24] Thus, in the present work, a colorimetric and paper-based sensor for the determination of As(III) and Pb(II) in environmental water samples is investigated.

A number of metal nanomaterials have recently been commonly used as sensing probes for the detection of multiple analytes in food, pharmaceutical, environmental, and biological samples due to environment-friendly and low-cost considerations.[25] This is due to the distinct optical properties of AuNPs (pink), AgNPs (yellow), and CuNPs (red) in aqueous solution, which cause LSPR absorption band in the UV-Vis spectrum. The LSPR of noble metal NPs is related to the conduction of free electrons present in the valence band after interaction with visible light and is dependent on the size of the NPs.[26] However, the introduction of analytes into the NPs solution can cause the agglomeration of particles, which results in the change of color and the red shift of the LSPR band to longer wavelength in the visible region. LSPR-based probes are able to detect extremely low concentration of the analytes present in different types of samples.[27,28] Consequently, noble metals NPs are used as colorimetric and paper-based sensors for the detection of a variety of chemical substances such as amino acids,[29] vitamins,[30] pesticides,[31–33] proteins,[34] cationic surfactants,[35] nucleic acids,[36] and ascorbic acid.[37,38] Thus, colorimetric and paper-based analytical methods based on noble AuNPs are easy, low cost, and preclude the use of sophisticated analytical instruments.

In the present work, a simple method for the selective determination of As(III) and Pb(II) in environmental water samples was developed using glucose-functionalized AuNPs as a colorimetric and paper-based sensor under the optimized conditions. The methodologies are based on the non-covalent interaction of the analytes and AuNPs/Glu, followed by the shifting of the LSPR band in the visible region. The effects of concomitant ions and cross-contaminants were also studied for the selective determination of As(III) and Pb(II) using the NPs in water samples. The linearity range, accuracy, precision, and limit of detection of the present method were calculated and validated for the determination of As(III) and Pb(II) in water samples. Finally, AuNPs/Glu was applied for As(III) and Pb(II) determination in environmental water samples (bore-well, industrial waste, river, and pond water) the using paper-based colorimetric sensor.

2. Materials and methods

2.1. Chemicals, reagents, and solution preparations

All reagents and materials used were of analytical grade for the experimental process. The different metal salts were purchased from S.D. Fine Chemical Ltd. (Mumbai, India). Glucose, chloroauric acid ($AuHCl_4$), and trisodium citrate were obtained from Hi-Media (Mumbai, India). Glass microfiber filter paper, Whatman filter paper, chromatography filter paper, and quartz filter paper were purchased from Whatman (International Ltd, Maidstone England). Xerox printing paper and tissue paper were purchased from a local market and were used for AuNPs/Glu fabrication on the surface of the paper-devices for the selective detection of As(III) and Pb(II). Stock solutions (1000 μg L^{-1}) of all the metal ions were prepared by dissolving a proper amount of the substance in 10 mL of ultrapure water. The working standard solutions were prepared by the manyfold dilution of the standard stock solution. 0.1 M solutions of hydrogen chloride (HCl) and sodium hydroxide NaOH (ACS reagent, 97%, Sigma-Aldrich) were prepared for maintaining the pH of the sample solutions, which were added to the reaction medium.

2.2. Synthesis of modified gold nanoparticles

AuNPs/Glu was prepared by the reduction of $AuHCl_4$ using trisodium citrate as the reducing agent and glucose as the stabilizing agent.[39] 40 mL of 195 μM aqueous solution of $HAuCl_4$ was warmed to 100 °C and then 540 μL of trisodium citrate (0.1 M) was added immediately into the stirred mixture of the solution in a 100 mL conical flask. The pink color appearance of the solution mixture showed the formation of the AuNPs without stabilizing agents. At the same temperature, the solution mixture was heated for 2 hours and centrifuged for 15 min (12 000 rpm) to extract excess of trisodium citrate from the dispersed medium of AuNPs and mixed with ultrapure water accordingly. Next, a 0.5 mL of glucose solution (0.05 mM) was introduced into 40 mL of the above prepared AuNPs, followed by sonication for ligand exchange reaction. After this, the nanoparticles were centrifuge at 12 000 rpm for 15 min to eliminate any additional ligands from the solution mixture. AuNPs/Glu was found to be stable for 5 months at room temperature with no signs of aggregation, indicating that it could be used as a chemical sensor in paper-based and colorimetric methods.

2.3. Sample collection and preparation

The water samples were collected from different sources such as bore-well, industrial waste, river, and pond from Chhattisgarh, India. In the month of December 2020, the samples were collected in polyethylene bottles using the prescribed methodology.[35] The samples were immediately filtered through a Whatman filter paper (0.45 μm) to prevent the adsorption of any chemical species on the surface of the suspended elements and kept in a freezer at 5 °C in 24 h until analysis. The pH of the sample was maintained at 7.0 prior to the AuNP/Glu-assisted colorimetric and paper-based analysis.

2.4. Procedure for the determination of As(III) and Pb(II) using AuNPs/Glu in the colorimetric and paper-based sensor

Standard solutions of As(III) and Pb(II) from 200 μL were separately placed in glass bottles containing 1.0 mL of AuNPs/Glu

and filled with the appropriate dilution of the stock standard solution while maintaining the pH of the sample solution at 7.0 with the help of 0.1 M aqueous solutions of NaOH and HCl. The solution mixture was then kept at room temperature to study the chemical reaction as well as the color change of the nanoparticles. The color of the sample solution suddenly changed from pink to purple for As(III) and from pink to bluish grey for Pb(II). The change in the color of the solution mixture can be seen with the naked eye and the signal intensity of the solution mixture was measured with a UV-Vis spectrometer in between the 200–800 nm range.

For paper-based detection, glass microfiber filter paper was punched into small diameter (0.5 cm) circles and stacked on the paper substrate with a hydrophobic surface wax. On each paper substrate with the help of a micropipette, 10 μL of AuNPs/Glu was deposited, followed by 10 μL of As(III) and Pb(II) with concentrations in the range of 20–500 μg L^{-1} and 20–1000 μg L^{-1}, each of them being added. The color change observed of the detection zone of the paper substrate with As(III) and Pb(II) from pink to violet for both the analytes was used in the quantitative and qualitative analysis of both the metal ions from contaminated sample sites. The schematic diagram for the determination of As(III) and Pb(II) using AuNPs/Glu in the paper-based and colorimetric sensor is shown in Fig. 1.

A standard calibration curve of different concentrations of As(III) and Pb(II) was prepared simultaneously by our performing different sets of experiments in six replicates of analyses by the paper-based and colorimetric method. The calibration curve was drawn between different concentrations of As(III) and Pb(II) and their respective absorbance or value of color intensity using the linear calibration curve equation, *i.e.*, $y = mx + c$.

2.5. Apparatus

The LSPR absorption intensity was used to determine As(III) and Pb(II) in standard solution/water samples using the UV-visible spectrometer (Cary-60, Agilent Technologies, USA) with 1 cm of cell made up of quartz. The pH of the sample solution was measured using a digital pH meter (model-335, Systronics, India). The size and shape of AuNPs/Glu were determined using a transmission electron microscope (TEM) (Jeol, IET-2200FS) with a 100 kV accelerating voltage in the presence and absence of target analytes. The infrared (IR) absorption spectra of pure glucose, AuNPs/Glu, and AuNPs/Glu with As(III) and AuNPs/Glu with Pb(II) were obtained using a Fourier transform infrared spectrometer (FTIR) (Nicolet-iS10, Thermo Scientific, USA). Dynamic light scattering Nano-Zetasizer instrument (Malvern, UK) confirmed the percentage size distribution of the nanoparticles in aqueous solution before and after the addition

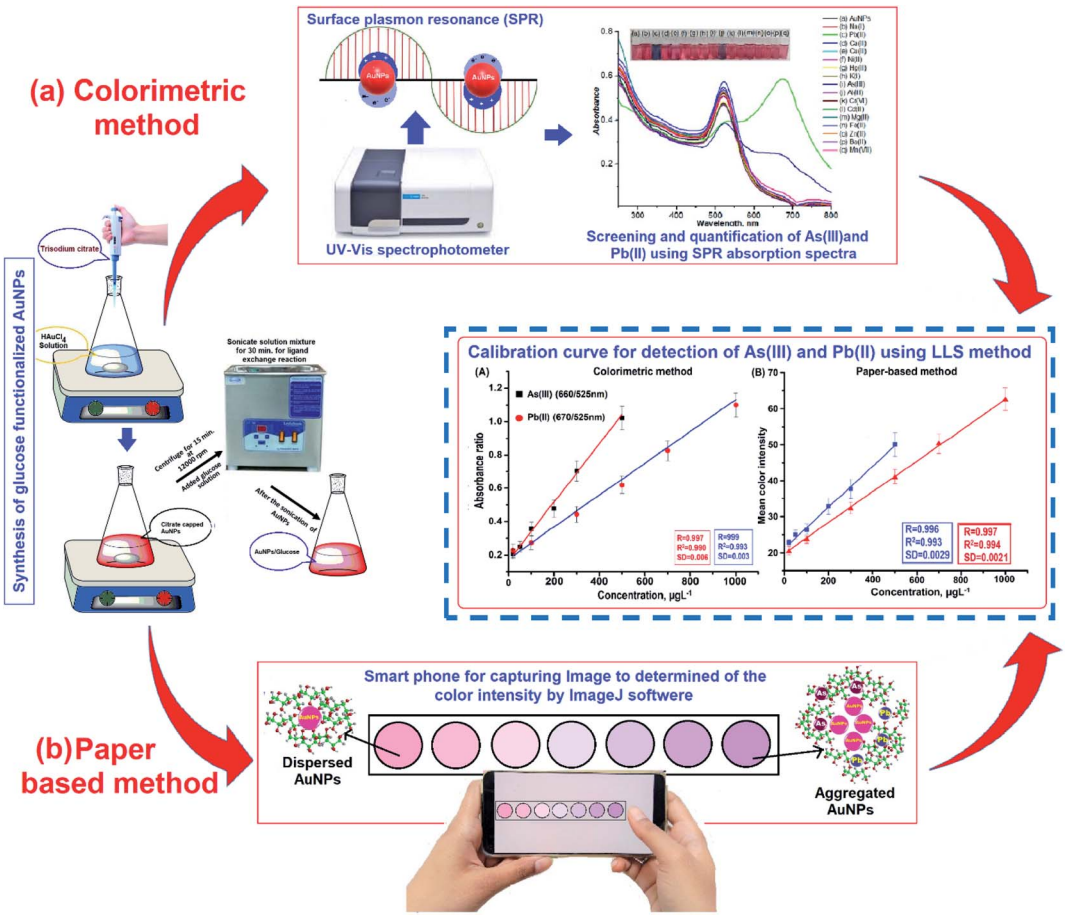

Fig. 1 Schematic representation for the LSPR-based colorimetric method (a) and smartphone-assisted paper-based sensor by processing in the ImageJ software (b) for the determination of As(III) and Pb(II) using AuNPs/Glu.

of As(III) and Pb(II). Thermo Fisher Scientific Barnstead Smart2pure water system with a conductivity of 18.2 Ω^{-1} was used to obtain ultrapure water for the solution preparation of all chemical compounds.

3. Results and discussion

3.1. Selection of functionalized nanoparticles and paper for sensing materials

In this present method, we have chosen glucose-functionalized AuNPs for the detection of As(III) and Pb(II) in environmental water samples because it shows chemical stability and size-dependent optical and electronic properties.[40] Generally, AuNPs have a large surface area-to-volume ratio, excellent biocompatibility, and low toxicity, which is an important decisive factors for the selection as well as better adsorption of As(III) and Pb(II) on the surface of nanoparticles and they have been used in a gamut of applications, including antibacterial agents, biosensing, biomedical, and bioremediation of diverse contaminants and water treatments.[41,42] The enhancement of the signal intensity in UV-Vis analysis as well as the red shift of the LSPR band in the UV-Vis region confirmed the functionalized AuNPs as the better chemical probe as compared to other nanoparticles. AuNPs are more chemically stable than AgNPs and can be stored for a long time. In contrast, AgNPs are very susceptible to oxidation when exposed to air and light.[35] The selection of the paper is important for the development of paper-based sensors towards the determination of As(III) and Pb(II) from different types of environmental water samples. Glass microfiber filter paper with and without nanoparticles were examined for the determination of As(III) and Pb(II) due to the high signal intensity as compared to Whatman filter, quartz filter, and xerox printing paper. Except for glass microfiber filter paper, the quartz filter, Whatman filter, and xerox printing paper were found to be unsuitable since the very large pore size on their surface led to the incomplete trapping of the analytes within the fibers of the paper due to the rapid spreading of the liquid, resulting in a low color appearance.[43] Therefore, AuNPs were used for the multiresidue detection of metal ions (As(III) and Pb(II)) using glass microfiber filter based paper sensor and colorimetry in environmental water samples.

3.2. Characterization of colloidal nanoparticles

The current study used a variety of instruments to investigate the morphology, size distribution, and spectral characteristics of the synthesized AuNPs/Glu under the optimum conditions. For the characterization, a UV-vis spectrophotometer was firstly used for AuNPs/Glu size determination with and without the addition of analytes and it was analyzed by observing the shifting of the LSPR absorption band. Good intense pink color and UV-visible absorption spectra were only observed in AuNPs/Glu and not in other nanoparticles functionalized with different compounds (Fig. S1†). The solid-state UV-VIS spectra of the test paper with and without arsenic(III) and lead(II) are shown in Fig. S2.† The good chemical stability of AuNPs/Glu was observed due to surface functionalization by negatively charged hydroxyl ions, which avoid self-aggregation of the nanoparticles. Secondly, TEM analysis was used to confirm the particle size of AuNPs/Glu with and without the addition of the analyte. It is evident for the currently synthesized AuNPs using glucose as the stabilizing agent from the TEM images that in the absence of metal ions (As(III) and Pb(II)), the AuNPs were spherical in shape, monodisperse in nature, and well-dispersed in aqueous solution. Fig. 2A displayed the TEM image of AuNPs/Glu without and with the addition of metal ions such as As(III) and Pb(II). The FTIR absorption of dispersed AuNPs/Glu and aggregated AuNPs/Glu with As(III) and Pb(II) was performed on the basis of the functional groups, chemical bonding, and molecular

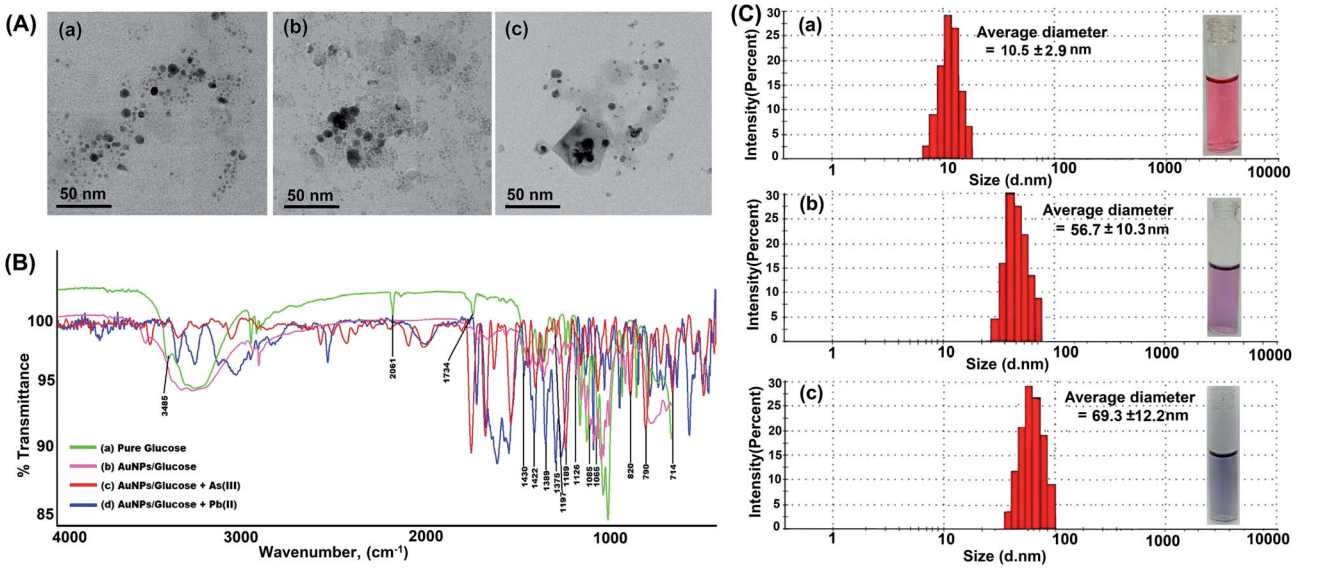

Fig. 2 (A) TEM image of (a) disperse AuNPs/Glu, (b) aggregate AuNPs/Glu with As(III), (c) aggregate AuNPs/Glu with Pb(II); (B) FTIR spectra of (a) pure glucose and (b–d) AuNPs/Glu with and without the addition of As(III) and Pb(II); (C) DLS measurement histogram of (a) the size distribution of AuNPs/Glu and (b, c) AuNPs/Glu with and without the presence of metal ions such as As(III) and Pb(II).

structures of the chemical substances. The results are shown in Fig. 2B. DLS was also performed to confirm the average size and percentage distribution of AuNPs/Glu with and without the addition of As(III) and Pb(II) in aqueous solution, and the results are displayed in Fig. 2C(a)–(c).

3.3. Screening for the selective detection of As(III) and Pb(II) using AuNPs/Glu in the colorimetric and paper-based sensor

Recently, our research group has exploited the use of paper-based and colorimetric sensor for the quantitative analysis of metal ions using functionalized NPs based on the discoloration of NPs, which impregnated the paper substrate, and the red shift of localized surface plasmon resonance (LSPR).[43] In this present work, different metal ions (Na(I), K(I), Ca(II), Co(II), Ni(II), Cu(II), Zn(II), Cd(II), Ba(II), Hg(II), Fe(III), and Cr(VI)) were chosen to demonstrate the selective detection of As(III) and Pb(II) with AuNPs/Glu in environmental water samples using a colorimetric probe. For this analysis, standard solutions of different metal ions (200 μL) were taken in separate glass vials and mixed with 1.0 mL of colloidal gold solution. After that, the pH of the sample solution was maintained at 7.0 with 5 min reaction time. The color of the AuNPs/Glu solution changed from pink to purple and pink to bluish grey, and the shift in the LSPR band was appearance due to the aggregation of the particles after the addition of As(III) and Pb(II) and not with other metal ions, respectively (Fig. 3(A), (C)). Thus, the change in the solution color and appearance of a new LSPR band at 660 nm for As(III) and at 670 nm for Pb(II) with AuNPs/Glu were used as a paper-based and colorimetric assay method for the selective determination of target analytes in environmental water samples. The LSPR absorption peak of the AuNPs/Glu solution with all other metal ions was found to be close to the UV-vis spectrum of AuNPs/Glu at 525 nm. However, when As(III) and Pb(II) were added to the AuNPs/Glu solution, a new LSPR absorption band and high signal intensity or signal-to-noise ratio appeared at about 660 nm and 670 nm, respectively, as compared to other metal ions. As a result, the change in the color and appearance of the new LSPR absorption band at 660 nm and 670 nm for As(III) and Pb(II), respectively, are shown in Fig. 3A. Therefore, AuNPs/Glu was used as a colorimetric and paper-based sensor for selectively determining both the metal ions in environmental samples based on the agglomeration of dispersed nanoparticles.

The screening of metals ions was performed for the selective determination by depositing 200 μL of different metal ions (1000 μg mL^{-1}) on the surface of the paper substrate fabricated with AuNPs/Glu for the determination of As(III) and Pb(II), as shown in Fig. 3B(a)–(q). The nanoparticles that contain As(III) and Pb(II) ions (Fig. 3B(c) and (j)) only showed a change in the color from pink to violet for both As(III) and Pb(II), respectively, and no changes in the color were observed with another metal ions, which is shown in Fig. 3B and (C). Apart from this, the deposition of different metal ions on the paper substrate exhibited the same color as AuNPs/Glu, showing that there might not be any interaction of these metal ions with NPs. As is known, all paper substrates including glass microfiber filter paper possess pores with a diameter of 2–20 mm on their surface, which is an important criterion for the adsorption of analytes, resulting in an increase in the color intensity. The lowest background and high signal intensity of the target analytes were obtained with the microfiber filter paper due to electrostatic interaction in the solid–liquid interfaces.[43] In addition, the control experiment was performed to determine the variation of signal intensity after the deposition of AuNPs/Glu on the surface of another paper. The results indicated that there is no significant change in the variation of the signal intensity between different paper substrates for the analysis of metal ions such as As(III) and Pb(II). Thus, the results from the ImageJ software confirmed the qualitative data for the determination of As(III) and Pb(II) using a smartphone coupled with the paper sensor. We have also experimentally observed that the same color change was found in the UV-Vis analysis of AuNPs as a colorimetric sensor. Therefore, AuNPs/Glu can be fabricated on a paper substrate for the colorimetric qualitative determination of As(III) and Pb(II) from a sample solution.

3.4. Mechanism for the detection of As(III) and Pb(II) using AuNPs/Glu as the chemical sensor

The mechanism for the selective detection of metal ions such as As(III) and Pb(II) using AuNPs/Glu was demonstrated by performing different sets of experiments with and without the use

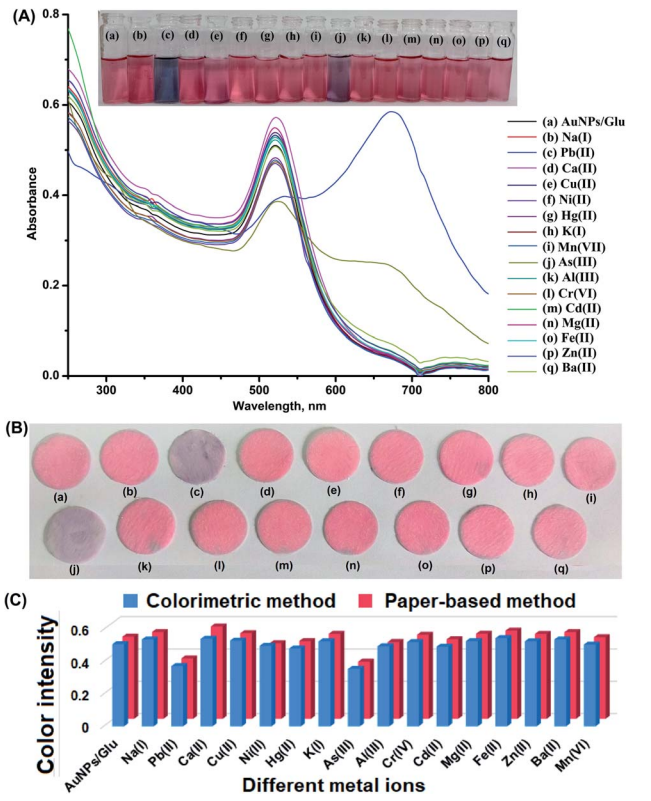

Fig. 3 Images of glass vials containing solution mixtures of different metal ions with AuNPs/Glu and their respective UV-visible spectra (A), photographs of paper strips (B) and histogram plotted between different metal ions and color intensity for the screening and selective determination of As(III) and Pb(II) in water samples (C).

of colloidal gold solution in the paper sensor and the colorimetric method. AuNPs/Glu shows the good dispersion of particles in the aqueous solution (pink color). This is because of the occurrence of oxygen and hydroxyl group in glucose molecules on the surface of NPs, which protect them from self-agglomeration. AuNPs/Glu showed a sharp LSPR absorption band at about 525 nm, as shown in Fig. S1(a).† The appearance of the LSPR absorption peak at 525 nm confirmed the size of NPs in the range of 10–50 nm.[44,45] However, the addition of As(III) and Pb(II) into the NPs solution caused the color change from pink to purple and from pink to bluish grey, respectively. Hence, a red shift was obtained from 525 nm to 660 nm for As(III) and from 525 nm to 670 nm for Pb(II) were due to the aggregation of particles, as shown in Fig. S1(b) and (c).† The aggregation of NPs causes a decrease in the inter-particle distance among the particles, followed by strong enhancement of localized electric field, which produces a red shift in the LSPR band at about 660 nm for As(III) and 670 nm for Pb(II) in the visible region, as shown in Fig. S1(b) and (c).† The aggregation of particles was evidenced by a color change of NPs from pink to purple and from pink to bluish grey after the introduction of As(III) and Pb(II) into the AuNP/Glu solution. The discoloration of AuNPs/Glu due to the aggregation of particles after the addition of the analyte on the paper surface was found because the paper still has fine glass microfibers.[46] In addition, the nature of SiO_4^{4-} in glass microfibers filter paper plays an important role in the adsorption of As(III) and Pb(II) at the solid–liquid interface due to the electrostatic interactions. Recently, our research group has been reported a KBr-impregnated paper substrate as a sample probe for the enhanced IR signal strength of surfactants in an aqueous medium with the same phenomenon.[43]

TEM measurement was also performed to verify the actual size, shape, and morphologies of AuNPs/Glu before and after the addition of As(III) and Pb(II) in aqueous solution. Fig. 2A shows the TEM image of AuNPs/Glu without the addition of As(III) and Pb(II) ions, displaying the monodispersity in aqueous solution. Fig. 2B(a)–(c) show the TEM images of the agglomerated NPs in the presence of the analyte and the average size of the NPs was found to be several folds higher than that of the dispersed NPs. We also determined the size and percentage distribution of AuNPs/Glu in the presence and absence of As(III) and Pb(II) using DLS measurements and the results are shown in Fig. 2C(a)–(c). An observation of Fig. 2C(a) showed that the size of AuNPs/Glu in the absence of metal ions (As(III) and Pb(II)) is 10.5 ± 2.9 nm. However, in the presence of analytes, the dynamic size of AuNPs/Glu increases from 10.5 ± 2.9 to 56.7 ± 10.3 nm for As(III) and 10.5 ± 2.9 to 69.3 ± 12.2 for Pb(II), as shown in Fig. 2C(b)–(c). The increase in the hydrodynamic diameter is attributed to analyte aggregation and a decrease in the electrostatic interaction between the analyte and AuNPs/Glu due to the chemical adsorption process.[47] The sizes of the NPs estimated from DLS, UV-Vis, and TEM were found to be consistent with each other. Hence, the monodispersed NPs exhibited pink color and the addition of the analyte into it caused the aggregation, followed by the color change and red shift of LSPR absorption. This phenomenon was exploited for the selective detection of As(III) and Pb(II) from the sample solution using AuNPs/Glu as a dual colorimetric sensing probe and paper-based sensor. The functionalization of AuNPs with glucose was verified by the FTIR spectra of pure glucose and AuNPs with glucose molecule. The results are shown in Fig. 2B(a). The FTIR spectral peak observed at 2061 cm^{-1} was due to C–H vibrations and 1734 cm^{-1} for C–O symmetric stretching.[48,49] The FTIR peaks observed at 1065 cm^{-1}, 1085 cm^{-1}, and 1126 cm^{-1} were due to functionalized AuNPs with glucose, as shown in Fig. 2B(b). The strong absorbance band found at 3303 cm^{-1} was due to the OH stretching of the glucose molecule. The absorption band of OH stretching undergoes a significantly high frequency shift observed at 3485 cm^{-1}, suggesting the intimate association between D-glucose and the surface of the AuNPs/Glu.[39] In addition, the decrease in the signal intensity observed compared to pure glucose confirmed the binding of C–O on the surface of the Au nanoparticles. Fig. 2B(c) shows the FTIR spectrum of AuNPs/Glu with As(III) observed at 714 cm^{-1}, 790 cm^{-1}, and 820 cm^{-1}.

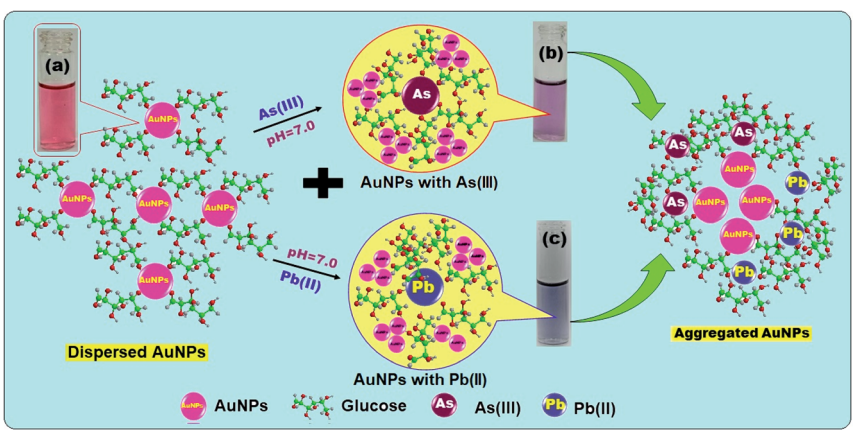

Fig. 4 Plausible mechanism for the detection of As(III) and Pb(II) ion using AuNP/Glu (a) glass vial containing pink color of the dispersed AuNPs/Glu, (b, c) glass vial containing purple and bluish grey color of the aggregated AuNPs/Glu with As(III) and Pb(II), respectively, due to the non-covalent interaction.

Fig. 2B(d) exhibits the FTIR spectrum of AuNPs/Glu with Pb(II) observed at 1430 cm^{-1}, 1422 cm^{-1}, and 1389 cm^{-1}. The peaks corresponding to As–O and Pb–O stretching frequency confirmed the binding of As(III) and Pb(II) to the surface of AuNPs/Glu. However, the solution mixture of AuNPs/Glu with As(III) and Pb(II) exhibited the decrease and the appearance of a broader band than that for glucose and AuNPs/Glu demonstrated the binding of the analyte with the glucose molecule.

Thus, the selective detection of As(III) and Pb(II) is illustrated based on the red shift of the LSPR absorption band of AuNPs/Glu after the introduction of the analyte using UV-Vis, TEM, and DLS analyses. The red shift of the band is due to the decrease in the inter-particle distance after the self-agglomeration of NPs compared to the monodispersed particles in aqueous solution. A similar effect on the formation of non-bonding interactions of the Pb(II) ion with a bifunctional gallic acid, leading to a strong inter-particle interaction of Au and AgNPs, was also proposed by Thomas and co-workers' research group (2010).[49] The sensing mechanism is based on the interaction of glucose from the surface of the AuNPs and glucose molecules with the breaking of Au–O interactions and stabilizing a new As–O. Similarly, non-covalent interaction is observed between the Pb(II) ion glucose-capped on the surface of the AuNPs. However, the solution mixture of AuNPs/Glu with As(III) and Pb(II) exhibited a decrease and the appearance of a broader band than that of pure glucose and AuNPs/Glu, which demonstrated the binding of the analyte with glucose molecules.

The schematic plausible sensing mechanism for the detection of As(III) and Pb(II) is designed based on experimental calculation (Fig. 4). The reaction between the analytes and AuNPs/Glu was completed in three steps for the determination of As(III) and Pb(II) (Fig. 5). Step-I indicates the synthesis of AuNPs using trisodium citrate as a reducing agent with the prescribed methodology.[39] The carboxylate group containing trisodium citrate was strongly adsorbed onto the colloidal AuNPs surface due to the interaction of the hydrogen bond, which provides stability to the colloidal nanoparticles in aqueous medium (Fig. 5). For the surface modification of AuNPs, we introduced the glucose as the functionalizing agent into the citrate-stabilized AuNPs, as shown in Step-II. As is known, glucose molecules have a majority of OH groups, which have strong affinity toward metal ions such as As(III) and Pb(II) in aqueous medium. In this process, we sonicated the solution mixture of NPs for the ligand exchange reaction (LER) for 15 min, resulting in the immediate removal of the excess ligands (carboxylate group of citrate molecules) from the solution mixture. At the same time, the hydroxyl ion (–OH) of glucose molecule binds with the colloidal gold solution due to ionic interaction and provides better stability to the AuNPs as compared to the carboxylate group containing citrate molecules (Fig. 5). In addition, the glucose-stabilized AuNPs prevents the self-induced aggregation of NPs with other ionic compounds. Therefore, the terminal part of glucose on the surface of NPs binds with the Au–O bond to form surface-modified AuNPs due to the interaction of the hydrogen bond in aqueous medium. The color change of AuNPs/Glu due to the addition of metal ions such as As(III) and Pb(II) samples can be interpreted by electrostatic as well as non-covalent interactions between As(III) and Pb(II) and AuNPs/Glu (Step-III). The glucose molecules were perpendicular to the surface of the AuNPs attached with the hydroxyl ion (OH) bond and these NPs gain a tunable negative

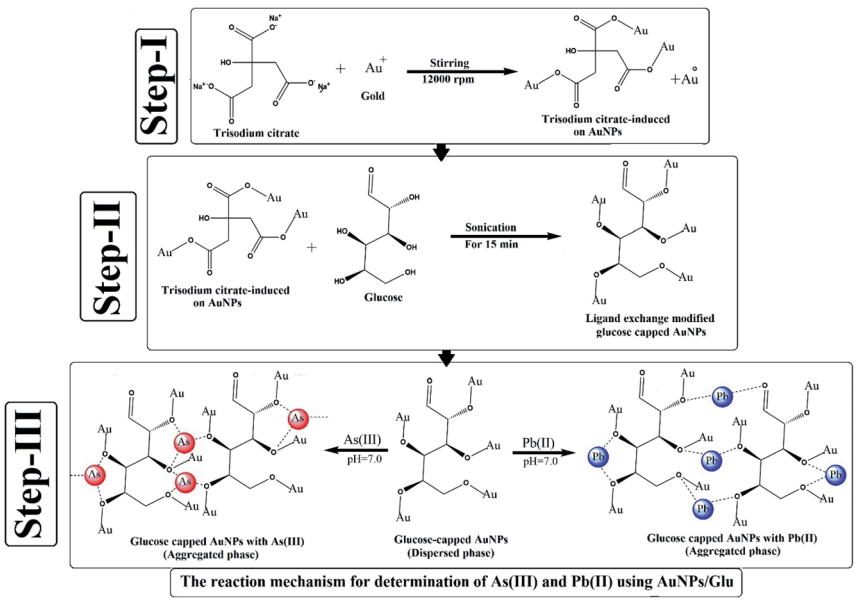

Fig. 5 Probable reaction pathways step-I indicates that the terminal carboxylate group of trisodium citrate binds on the surface of the NPs through the Ag–O bond, step-II indicates that the carboxylate group was replaced by glucose molecule and the terminal hydroxyl part of glucose binds to the surface of the AuNPs, and step-III shows that As(III) and Pb(II) containing positive charge (+ve) interact with the negative charge (–ve) site of the oxygen (O–H) of the hydroxyl group of glucose-functionalized AuNPs due to the agglomeration of particles for the determination of As(III) and Pb(II) using AuNPs/Glu.

surface charge. When these negative surface charged NPs come into contact with the positive charge of both the metal ions such as As(III) and Pb(II) during the electrostatic and non-covalent interactions. Due to the interaction of –OH groups and As(III) and Pb(II), electrostatic attraction takes place between AuNPs, which leads to their eventual aggregation, resulting in the reduction in the inter-particle distance (Fig. 5).[50,51] When the glucose molecule is left at the surface of the AuNPs, their stability decreases and they are found to self-aggregate, causing color change and also the shifting of the LSPR band in the visible region interact with this metal ion in the AuNPs. AuNPs capped with glucose in aqueous solution exhibited pink color due to the monodispersity of the particles achieved by the long carbon chain of glucose molecules.[51–53] The long carbon chain of glucose prevented the NPs from aggregation due to the steric hindrance, as shown in Fig. 4a. Thus, the LSPR absorption band of the NPs capped with glucose was observed at about 525 nm in the visible region. However, the addition of As(III) and Pb(II) into the NPs showed color change from pink to purple and bluish grey, respectively, because of the agglomeration of particles caused due to the binding of glucose molecules with the analytes, as shown inFig. 4b and c. This is due to the non-covalent interaction between the glucose molecules and As(III) as well as Pb(II) ions; therefore, the red shift of the LSPR band was observed from 525 to 660 nm for As(III) and 670 nm for Pb(II) in the visible region. The change in the color intensity and the red shift was found proportional to the concentration of the analytes, which was then used for the colorimetric analysis of As(III) and Pb(II) from the sample solution.

3.5. Determining factors for the performance of the colorimetric method using AuNPs/Glu

The methodology was optimized by investigating the effect of some analytical parameters that affect the detection as well as quantification of As(III) and Pb(II) using AuNPs/Glu as a chemical sensor in the colorimetric method such as reaction time, pH, and AuNPs concentration. Firstly, the pH of the solution was optimized by adding different pH solutions (3.0, 5.0, 7.0, 9.0, and 11.0) containing As(III) and Pb(II) ions, followed by the addition of nanoparticles, which is shown in Fig. S3 and S4.† The solution containing pH 7.0 demonstrates the highest absorption as well as color changes and thus the whole experiment retained this pH. The reaction time was then optimized by maintaining the solution mixture of the nanoparticles with As(III) and Pb(II) at room temperature for various reaction times, which is shown in Fig. S5 and S6.† After 5 minutes, there was no significant effect of the reaction time on As(III) and Pb(II)

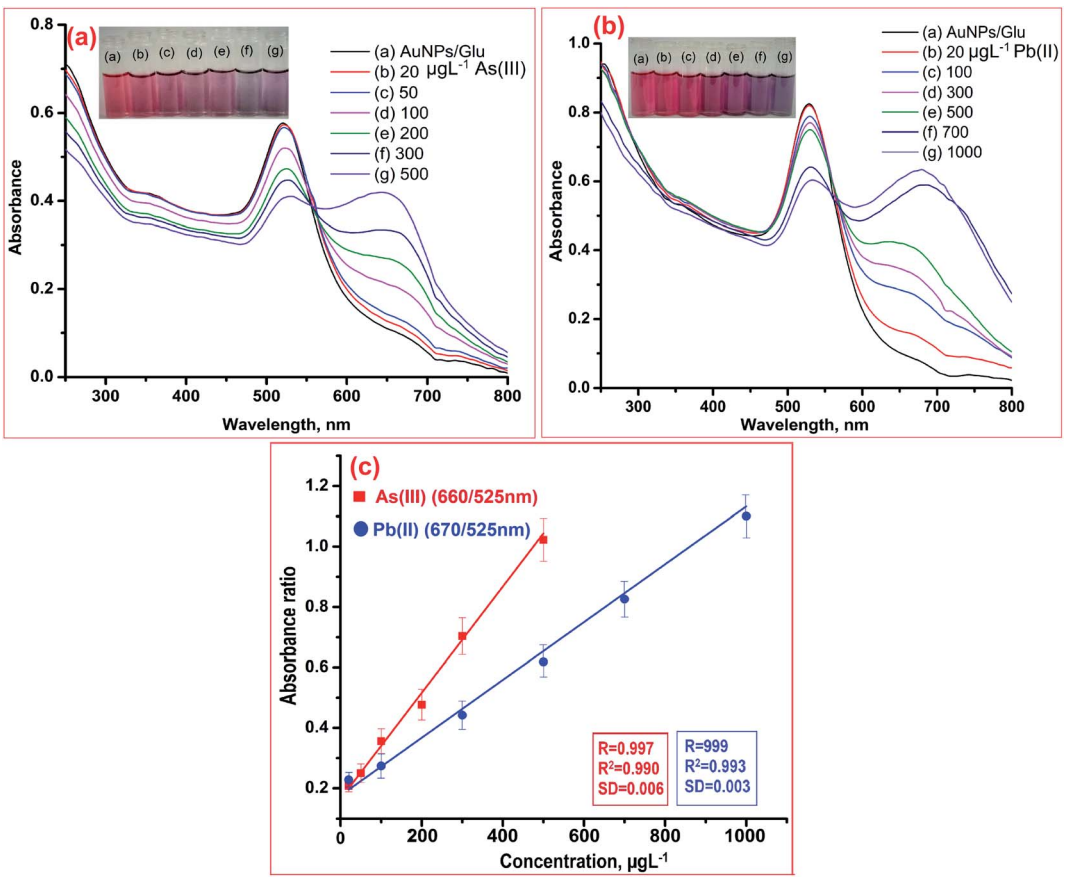

Fig. 6 Glass vials containing different concentration of (20, 50, 100, 200, 300, 500 μg L^{-1}) for As(III) and (100, 300, 500, 700, and 1000 μg L^{-1}) for Pb(II) with AuNPs/Glu and their respective UV-Vis absorption spectra (a, b) and the calibration curve for the determination of As(III) and Pb(II) in environmental water samples (c).

detection. Furthermore, different concentrations of the nanoparticles were optimized by recording the different absorbance at different concentrations of the nanoparticles in the range of 50–600 μM. The results are given in Fig. S7 and S8.† The absorbance value increased as the concentration increased from 50 to 500 μM but there was no improvement in the ΔA value beyond this point. Consequently, 200 μM concentrations of AuNPs were used for further investigation in order to detect both the target analytes. Finally, all the experiments were carried out by keeping the sample solution at pH 7.0 for 5.0 min reaction time and using 200 μM concentration of the NPs for the optimum detection of As(III) and Pb(II) from the sample solution.

3.6. Selectivity studies: effects of concomitant ions and cross-contaminants

Several metal ions such as K(I), Na(I), Mg(II), Ca(II), Mn(II), Co(II), Ni(II), Zn(II), Cu(II), Cd(II), Ba(II), Pb(II), Hg(II), Al(III), Fe(III), As(III), and Cr(IV), and also anions such as Cl^-, CO_3^-, NO_3^-, PO_4^{3-}, and SO_4^{2-} that may be found in water samples were examined using AuNPs/Glu in the colorimetric probe under optimum conditions. For this study, the determination of As(III) and Pb(II) using AuNPs/Glu was carried out by introducing water spiked with different concentrations of diverse metal ions, anions at pH 7.0, and an extraction time of 5 min, which was analyzed *via* the colorimetric probe. Different diverse substances with their tolerance limit such as K(I), Na(I), Zn(II), Cr(IV), Cl^-, CO_3^- (800 mg L^{-1}); Mn(II), Co(II), Ni(II), Al(III), SO_4^{2-} (750 mg L^{-1}), Hg(II), Mg(II), Ba(II), Ca(II), NO_3^- (650 mg L^{-1}); Cd(II), Cu(II), Fe(III), PO_4^{3-} (450 mg L^{-1}), were calculated using this method. Table S1† indicates the tolerance limit for metal ions and anions. The UV-Vis absorption band of AuNPs/Glu remained unchanged in the presence of other vitamins and amino acids at the optimized conditions, while only As(III) and Pb(II) displayed a decrease in the color change as well as the red shift of the LSPR absorption band (Fig. 3(A) and (C)). The ratio of absorbance intensities at 525/660 nm for As(III) and 525/670 nm for Pb(II) were used to assess the degree of AuNPs/Glu aggregation in the colorimetric probe for the determination of metal ions (As(III) and Pb(II)) from different water samples such as bore-well, industrial-waste, river, and pond. Thus, all the added chemical substances in water samples did not show interference in the determination of both As(III) and Pb(II), which shows the better selectivity of the AuNPs based on the colorimetric probe.

3.7. Analytical evaluation for the determination of As(III) and Pb(II) using AuNPs/Glu in the colorimetric and paper-based sensor

Linear range, limit of detection (LOD), precision, and accuracy for the determination of As(III) and Pb(II) in water samples were investigated at the optimized conditions. The calibration for the estimation of As(III) and Pb(II) was performed by mixing different concentrations of the target metal ions with 1.0 mL of AuNPs/Glu. After the addition of the analyte with different concentrations in the NPs solution, the aggregation and LSPR absorption intensity of the NPs solution mixture is influenced. A calibration curve was drawn by the absorbance ratio obtained at 660 nm for As(III) and 670 for Pb(II) and 525 nm against different concentration of the metal ions. A good linearity was obtained in the range of 20–500 μg L^{-1} (As(III)) and 20–1000 μg L^{-1} (Pb(II)) for the determination of both the metal ions with a correlation coefficient of 0.991 and 0.993, respectively, as shown in Fig. 6(a)–(c). The LOD was evaluated based on the minimum quantity of the analyte that could give a change in the absorbance value at three times the standard deviation value of the blank.[54,58] The LOD value for the detection of As(III) and Pb(II) was to be found to 5.6 μg L^{-1} and 7.7 μg L^{-1}, respectively. Thus, good results were obtained in terms of the sensitivity of LOD and reproducibility for the determination of As(III) and Pb(II) in the water samples using the present method. A good stability in aqueous solutions could be verified by the analyses of As(III) and Pb(II) using AuNPs/Glu as a chemical sensor for a minimum period of 35 days. For this, we calculated the intra-day precision (RSD%) for the analysis of As(III) and Pb(II) (200 μg L^{-1}) at the optimized condition for 35 days. The reproducibility curve for the determination of As(III) and Pb(II) using AuNPs/Glu under the optimized conditions is shown in Fig. S9.† The RSD% value in the range of 0.9–2.2% showed the better stability of the AuNPs/Glu for the effective detection of both the metal ions from the sample solution.

Consequently, the calibration was carried out by depositing different concentrations of As(III) and Pb(II) in the range of 20–500 μg L^{-1} and 20–1000 μg L^{-1} on different test zones of the circular paper fabricated with AuNPs/Glu. The results are given in Fig. 7a and b. The color of the AuNPs/Glu fabricated on paper changes from the pink to violet as the concentration of the

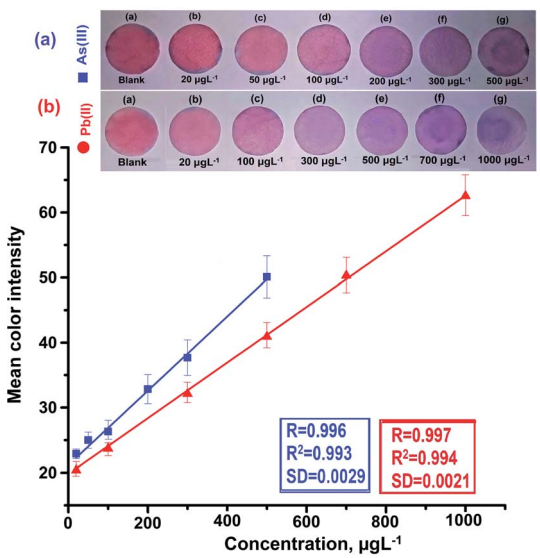

Fig. 7 (a) Circular filter paper strip fabricated with AuNPs/Glu along with the deposition of different concentrations of As(III): (a) AuNPs/Glu (blank), (b) 20 μg L^{-1}, (c) 50 μg L^{-1}, (d) 100 μg L^{-1}, (e) 200 μg L^{-1}, (f) 300 μg L^{-1}, and (g) 500 μg L^{-1} with the calibration curve; (b) circular filter strip fabricated with AuNPs/Glu along with the deposition of different concentrations of Pb(II): (a) AuNPs/Glu (blank), (b) 20 μg L^{-1}, (c) 100 μg L^{-1}, (d) 300 μg L^{-1}, (e) 500 μg L^{-1}, (f) 700 μg L^{-1}, and (g) 1000 μg L^{-1} with their calibration curve.

Table 1 Application to the determination of As(III) and Pb(II) in bore-well, industrial waste, river, and pond water samples[a]

Samples	As(III), μg L^{-1} ($n = 3$)	RSD, %	AAS, μg L^{-1} ($n = 3$)	RSD, %	Pb(II), μg L^{-1} ($n = 3$)	RSD, %	AAS, μg L^{-1} ($n = 3$)	RSD, %
Bore-well water, Bilaspur	122.1 ± 2.7	2.2	141.6 ± 2.0	1.4	304.6 ± 4.5	1.4	272.6 ± 2.5	0.9
Industrial waste water, Sarona	ND	ND	ND	ND	254.3 ± 4.0	1.5	224 ± 3.6	1.6
River water, Ambagarhchowki	222.3 ± 2.5	1.1	203.6 ± 3.2	1.5	ND	ND	ND	ND
Industrial waste water, Urla	ND	ND	ND	ND	243 ± 2.6	1.0	264.3 ± 3.7	1.4
Pond water, Raipur	ND	ND	ND	ND	ND	ND	ND	ND

[a] ND = not detected.

analytes are increased. The paper-based detection of metal ions is based on the change in the signal intensity of AuNPs/Glu fabricated on a paper substrate after the deposition of the analyte using a smartphone, followed by processing with the ImageJ software. The standard addition of As(III) and Pb(II) on the paper substrate will be helpful in the qualitative determination of unknown concentration of the analytes in the given samples. Thus, the paper-based detection of As(III) and Pb(II) ions is found to be a simple, rapid, and cheap analytical device that requires a very low amount of the sample and can be applied at the sample source.

3.8. Application to the determination of As(III) and Pb(II) using AuNPs/Glu from water samples

The validity of the AuNPs-based colorimetric probe was tested by determining As(III) and Pb(II) in bore-well, industrial waste, river, and pond water samples. The concentration of the metal ions was determined using standard calibration curves of As(III) and Pb(II). The concentration of As(III) and Pb(II) obtained from bore-well, industrial waste, river, and pond water samples were in the range of 122–222 μg L^{-1} and 243–306 μg L^{-1}, respectively. The results are given in Table 1. The obtained results demonstrated efficient and simple determination of As(III) and Pb(II) from different environmental samples using AuNPs as the colorimetric probe. The results obtained colorimetrically were validated by analyzing with AAS (Thermo Scientific iCE 3000 AAS). The results are given in Table 1. The comparable results were acquired with both the newly developed method and the AAS method. Therefore, AuNPs/Glu was successfully illustrated for the determination of As(III) and Pb(II) in different types of water samples. The same samples were also tested for the qualitative and quantitative analysis of As(III) and Pb(II) by introducing the sample solution on the test zones of the paper substrates. The color change from pink to violet color indicated the presence of the sample solution, which will be employed for the qualitative and quantitative analysis of both the metal ions from the contaminated sample source. The concentrations of As(III) and Pb(II) were found in the range of 20–25 μg L^{-1} and 10–20 μg L^{-1}, respectively. Therefore, AuNPs/Glu was successfully exploited for the determination of As(III) and Pb(II) in different types of water samples.

3.9. Comparison of the analytical features of the present method and other reported methods

The potential of the developed colorimetric probe using AuNPs/Glu is compared in terms of the linearity range and LOD for the

Table 2 Comparison of the proposed method with other reported NPs-based colorimetric methods for the determination of As(III) and Pb(II)

	As(III)		Pb(II)			
Methods	Linearity range, μM	LOD, μM	Linearity range, μM	LOD, μM	Samples	Ref.
AuNPs/surfactant	0.07–40.04	0.07	—	—	Drinking water	41
AuNPs/enzyme	—	—	0.07–0.70	0.0016	Environmental sample	42
AuNPs/DNAzyme-based	—	—	0.01–0.1	0.5	Biological sample	45
AuNPs/gallic acid	—	—	0.01–1.0	0.0093	Drinking water	49
Bare-AuNPs	0.07–6.67	0.03	—	—	Biological samples	50
AuNPs/citrate	0.05–1.33	0.02	—	—	Drinking water	51
AuNPs/polyethylene glycol (PEG)	0.07–0.27	0.07	—	—	Waste water	52
AuNPs/cationic polymer	0.05–0.8	0.02			Tap water and pond water	55
AuNPs	0.01–1.33	0.23	—	—	Water and cosmetics samples	56
AuNPs/papain	—	—	0–40	10	Lake water and tap water	57
AuNPs/Glu	0.02–0.5	0.05	0.02–1.00	0.07	Water samples	**Present method**

determination of As(III) and Pb(II) with other reported methods.[41,42,45,49–53,55–58] A wide linearity range and better LOD were obtained with the present method compared to the other reported methods (Table 2). The reason for the higher sensitivity is the use of AuNPs/Glu as a colorimetric probe for the detection of As(III) and Pb(II). However, the synthesis of AuNPs/Glu is found to be a single step and simple method, where a small amount of the sample solution is required, making it a cost-effective process compared to other methods for the detection of As(III) and Pb(II) from water samples. The linearity range, LOD, RSD, and recovery% values obtained by the newly developed AuNPs/Glu method were compared with the other reported methods for the determination of As(III) and Pb(II) in different types of samples. The LOD value obtained by the present method was found lower than obtained by UV-Vis spectrophotometry, fluorimetry, inductively coupled plasma hyphenated with mass spectrometry, and ATR-FTIR.[41,42,50,57] These earlier reported methods require a time-consuming sample preparation procedure, trained personnel, and high-cost chemical reagents.

4. Conclusion

Herein, we have successfully validated the highly efficient AuNPs/Glu as a colorimetric and paper-based sensor for the selective and sensitive determination of As(III) and Pb(II) in environmental water samples. AuNPs/Glu is very sensitive for the determination of As(III) and Pb(II) at the lowest concentration and can be easily detect by naked eyes due to the prominent color variation of the sample solution with and without the addition of analytes. The sensing mechanism for the determination of both the metals ions is dependent on the interaction of glucose with the surface of the AuNPs due to the non-covalent interaction with the break-down of the Ag–O bond and the formation of new As–O and Pb–O moieties. The routine analysis of metal ions is normally performed using sophisticated instruments such as AAS, ESI-MS, and AP-MALDI-MS, which are generally large in size, need trained personnel, require large quantity of chemicals and reagents, and involve time-consuming sample preparation processes. The currently developed colorimetric and paper-based methods are simple, cost effective, and provide a large surface area for better adsorption, leading to enhanced absorption bands in the visible region for the analysis. These methods were applied directly in the aqueous medium and do not require any other toxic reagents as compared to other reported method. The advantages of the colorimetric and paper-based probe are simplicity, lightweight, cost effectiveness, need of low amount of samples, and environmental friendliness. In the near future, the proposed method would be highly useful for the monitoring of others toxic metal ions in food, environmental, and biological samples.

Conflicts of interest

There are no conflicts to declare.

Acknowledgements

Bhuneshwari Sahu is thankful to Pt. Ravishankar Shukla University Raipur Chhattisgarh, India for providing a university scholarship under the VR. No. 1300/Fin-Sch./2019. The authors are grateful for financial assistant from UGC-SAP [No. F-540/7/DRS-II/2016 (SAP-I)] The one of author (K. Shrivas) are also thankful to Science and Engineering Research Board (SERB), New Delhi for Extra Mural Research Project (File No: EMR/2016/005813). Authors are thankful to the Head, School of Studies in Chemistry, Pt. Ravishankar Shukla University Raipur for providing laboratory facility.

References

1 J. T. Hou, J. L. Luo, S. X. Song, Y. Z. Li and Q. Z. Li, *Chem. Eng. J.*, 2017, **315**, 159–166.
2 X. L. Zhang, M. F. Wu, H. Dong, H. C. Li and B. C. Pan, *Environ. Sci. Technol.*, 2017, **51**, 6326–6334.
3 T. Shah, F. Munsif, R. D'amato and L. Nie, *Chemosphere*, 2020, **246**, 125766.
4 S. Banerjee, N. P. Kumar, A. Srinivas and S. Roy, *J. Hazard. Mater.*, 2019, **375**, 16–223.
5 L. Zaijun, Y. Yuling, T. Jian and P. Jiaomai, *Talanta*, 2003, **60**, 123–130.
6 Z. ZhaiQ and J. P. Zhang, *Asian J. Chem.*, 2013, **25**, 538–540.
7 M. Montperrus, Y. Bohari, M. Bueno, A. Astruc and M. Astruc, *Appl. Organomet. Chem.*, 2002, **16**, 347–354.
8 S. Bakırdere, D. Selali, C. Çağdaş, B. N. San and S. Keyf, *Anal. Lett.*, 2016, **49**, 1917–1925.
9 M. Schneider, H. R. Cadorim, B. Welza, E. Carasek and J. Feldman, *Talanta*, 2018, **188**, 722–728.
10 J. Chena, S. Xiaob, X. Wu, K. Fang and W. Liu, *Talanta*, 2005, **67**, 992–996.
11 K. Jitmanee, M. Oshim and S. Motomizu, *Talanta*, 2005, **66**, 529–533.
12 A. Väisänen, R. Suontamo, J. Silvonen and J. Rintala, *Anal. Bioanal. Chem.*, 2002, **373**, 93–97.
13 D. Pröfrock and A. Prange, *Appl. Spectrosc.*, 2012, **66**, 843–868.
14 D. S. Rodas, W. T. Corns, B. Chen and P. B. Stockwell, *J. Anal. At. Spectrom.*, 2010, **25**, 933–946.
15 B. Beltrán, L. O. Leal, L. Ferrer and V. Cerdà, *J. Anal. At. Spectrom.*, 2015, **30**, 1072–1079.
16 A. Salimi, H. Mamkhezri, R. Hallaj and S. Soltanian, *Sens. Actuators, B*, 2008, **129**, 246–254.
17 T. Zerihun and P. Gründler, *J. Electroanal. Chem.*, 1996, **415**, 85–88.
18 X. Li, J. Tian, T. Nguyen and W. Shen, *Anal. Chem.*, 2008, **80**, 9131–9144.
19 A. M. L. Marzo and A. Merkoçi, *Lab Chip*, 2016, **16**, 3150–3176.
20 A. W. Martinez, S. T. Phillips, M. J. Butte and G. M. Whitesides, *Angew. Chem., Int. Ed.*, 2007, **46**, 1318–1320.
21 G. H. Chen, W. Y. Chen, Y. C. Yen, C. W. Wang, H. T. Chang and C. F. Chen, *Anal. Chem.*, 2014, **86**, 6843–6849.

22 K. C. Noh, Y. S. Nam, H. J. Lee and K. B. Lee, *Analyst*, 2015, **140**, 8209–8216.
23 A. Apilux, W. Siangproh, N. Praphairaksit and O. Chailapakul, *Talanta*, 2012, **97**, 388–394.
24 N. Ratnarathorn, O. Chailapakul, C. S. Henry and W. Dungchai, *Talanta*, 2012, **99**, 552–557.
25 J. T. Hou, J. L. Luo, S. X. Song, Y. Z. Li and Q. Z. Li, *Chem. Eng. J.*, 2017, **315**, 159–166.
26 L. Chen, W. Lu, X. Wang and L. Chen, *Sens. Actuators, B*, 2013, **182**, 482–488.
27 N. E. Motl, A. F. Smith, C. J. De and S. E. Santisa, *Chem. Soc. Rev.*, 2014, **43**, 3823–3834.
28 J. P. Lafleur, S. Senkbeil, T. G. Jensen and J. P. Kutter, *Lab Chip*, 2012, **12**, 4651–4656.
29 K. A. Rawat and S. K. Kailasa, *Microchim. Acta*, 2014, **181**, 1917–1929.
30 L. Gong, B. Du, L. Pan, Q. Liu, K. Yang, W. Wang, H. Zhao, L. Wu and Y. He, *Microchim. Acta*, 2017, **184**, 1185–1190.
31 N. Xia, Y. Shi, R. Zhang, F. Zhao, F. Liua and L. Liu, *Anal. Methods*, 2012, **4**, 3937–3941.
32 B. Sankar, B. Biswas and R. Biswas, *Opt. Laser Technol.*, 2018, 1–5.
33 K. Shrivas, S. Sahu, B. Sahu, R. Kurrey, T. K. Patle, T. Kant, I. Karbhal, M. L. Satnami, M. K. Deb and K. K. Ghosh, *J. Mol. Liq.*, 2019, **275**, 297–303.
34 T. Kang, S. M. Yoo, M. Kang, H. Lee, H. Kim, S. Y. Lee and B. Kim, *Lab Chip*, 2012, **12**, 3077–3081.
35 K. Shrivas, Monisha, S. Patel, S. S. Thakur and R. Shankar, *Lab Chip*, 2020, **20**, 3996–4006.
36 K. Shrivas, N. Nirmalkar, S. S. Thakur, R. Kurrey and D. Sinha, *RSC Adv.*, 2018, **250**, 14–21.
37 S. Rostami and A. Mehdinia, *Spectrochim. Acta, Part A*, 2017, **180**, 204–210.
38 L. Shen, J. A. Hagen and I. Papautsky, *Lab Chip*, 2012, **12**, 4240–4243.
39 Y. M. Sung and S. P. Wu, *Sens. Actuators, B*, 2014, **201**, 86–91.
40 R. Kurrey, M. K. Deb, K. Shrivas, B. R. Khalkho, J. Nirmalkar, D. Sinha and S. Jha, *Anal. Bioanal. Chem.*, 2019, **411**, 6943–6957.
41 N. L. T. Nguyen, C. Y. Park, J. P. Park, S. K. Kailasa and T. J. Park, *New J. Chem.*, 2018, **42**, 11530–11538.
42 C. W. Lien, Y. T. Tseng, C. C. Huang and H. T. Chang, *Anal. Chem.*, 2014, **86**, 2065–2072.
43 R. Kurrey, M. K. Deb, K. Shrivas, J. Nirmalkar, B. K. Sen, M. Mahilang and V. K. Jain, *RSC Adv.*, 2020, **10**, 40428–40441.
44 K. Shrivas, B. Sahu, M. K. Deb, S. S. Thakur, S. Sahu, R. Kurrey, T. Kant, T. K. Patle and R. Jangde, *Microchem. J.*, 2019, **150**, 1–10.
45 H. Wei, B. Li, J. Li, S. Dong and E. Wang, *Nanotechnology*, 2008, **19**, 095501.
46 K. Abe, K. Suzuki and D. Citterio, *Anal. Chem.*, 2008, **80**, 6928–6934.
47 R. Kurrey, M. K. Deb and K. Shrivas, *New J. Chem.*, 2019, **43**, 8109–8121.
48 K. W. Huang, C. J. Yua and W. L. Tseng, *Biosens. Bioelectron.*, 2010, **25**, 984–989.
49 Y. Kong, J. Shen and A. Fan, *Anal. Sci.*, 2017, **33**, 925–930.
50 J. Entwisle and R. Hearn, *Spectrochim. Acta, Part B*, 2006, **61**, 438–443.
51 J. S. Zhang and C. Noguez, *Plasmonics*, 2008, **3**, 127–150.
52 R. Kurrey, M. Mahilang, M. K. Deb and K. Shrivas, *Trends Environ. Anal. Chem.*, 2019, **21**, e00061.
53 N. Xia, Y. Shi, R. Zhang, F. Zhao, F. Liua and L. Liu, *Anal. Methods*, 2012, **4**, 3937–3941.
54 F. Chai, C. Wang, T. Wang, L. Li and Z. Su, *ACS Appl. Mater. Interfaces*, 2010, **2**, 1466–1470.
55 R. Gunupuru, D. Maity, G. R. Bhadu, A. Chakraborty, D. N. Srivastava and P. Paul, *J. Chem. Sci.*, 2014, **126**, 627–635.
56 Y. Wu, S. Zhan, F. Wang, L. He, W. Zhi and P. Zhou, *Chem. Commun.*, 2012, **48**, 4459–4461.
57 Y. Brechbuhl, I. Christl, E. J. Elzinga and R. Kretzschmar, *J. Colloid Interface Sci.*, 2012, **377**, 313–321.
58 S. Megarajan, K. R. Kanth and V. Anbazhagan, *Spectrochim. Acta, Part A*, 2020, **239**, 118485.